Bacterial cellulose nanofibrils from a by-product of the growing Kombucha business: Obtention and use in the development of poly(lactic acid) composites

J. Bovi[1,2], M. Butto[1,2], S. Arroyo[1,3], C. Bernal[1,2] and M.L. Foresti[1,2,*]

[1]*Universidad de Buenos Aires. Facultad de Ingeniería. Buenos Aires, Argentina*
[2]*CONICET – Universidad de Buenos Aires. Instituto de Tecnología en Polímeros y Nanotecnología (ITPN). Buenos Aires, Argentina*
[3]*CONICET – Universidad de Buenos Aires. Instituto de Tecnologías y Ciencias de la Ingeniería "Hilario Fernández Long" (INTECIN). Buenos Aires, Argentina*
**Corresponding author*: mforesti@fi.uba.ar

ABSTRACT Bacterial cellulose nanofibrils were obtained from the floating pellicle developed at the air-liquid interface during Kombucha tea production. Kombucha-derived bacterial nanocellulose (KBNC) was purified by different treatments and characterized in terms of morphology, chemical structure, thermal decomposition pattern and crystallinity. Purified KBNC was then employed in the production of poly(lactic acid) (PLA)-based composites obtained by melt compounding and compression molding. The morphology and the mechanical properties of the composites with increasing contents of KBNC (*i.e.* 1, 3, 5, 7 wt.%) were analyzed. Results showed that KBNC was suitable for the development of PLA composites with improved stiffness.

KEYWORDS Bacterial nanocellulose; Kombucha tea; Poly(lactic acid); Biocomposites; Characterization

1. Introduction

Over the last decades, the increasing consciousness on the health implications of human diet has promoted the incorporation of several beneficial habits by an important fraction of society. In this context, general wellness is frequently associated with the preferential consumption of natural food and organic functional products. Among these products, in the last years some drinks such as Kombucha, –a sparkling acidic and sometimes slightly alcoholic ancient beverage produced by fermentation of tea (commonly black or green tea) by a consortium of microorganisms–, have gained high popularity due to the multiple functional properties attributed to their consumption. The Kombucha market is a particularly fast-growing segment in the functional beverage category (2.2 billion USD in 2021, over 5 billion USD forecasted for 2025, over 13 billion USD for 2030 (Andreson et al. (2022); Kim and Adhikari (2020); https://www.acumenresearchandconsulting.com/Kombucha-market), being its increasing worldwide consumption associated with a growing demand for organic, clean-label functional beverages, as well as multiple claimed (but not still sufficiently proved clinically) therapeutic effects, such as promotion of excretion of toxins, and antioxidant, antimicrobial, anti-inflammatory and antihypertensive properties (Dima et al., 2017; Dutta and Paul, 2019; Jayabalan et al., 2014).

Traditional Kombucha is produced by fermentation of sweetened tea using a *S*ymbiotic *C*ulture *O*f *B*acteria and *Y*east (SCOBY). Although it has a variable composition, acetic acid bacteria and yeasts are known to be the main components. Species from the genera of lactic acid bacteria have also been identified (Andreson et al., 2022). Yeasts ferment sugars to produce ethanol, and acetic acid bacteria do the conversion of ethanol and remaining sugars into organic acids (e.g. acetic acid, gluconic acid, glucuronic acid) (Laavanya et al., 2021). In the meantime, specific acetic acid bacteria produce a highly hydrated membrane that grows on the surface of the fermentation vial which is known to be mainly constituted by cellulose.

Cellulose, the most abundant biopolymer in nature, is highly recognized in the field of biobased materials due to its high stiffness and strength, low density, renewable character, biodegradability, biocompatibility, non-toxicity, high availability and relatively low cost. Besides, in the last decades, plant cellulose has received a renewed interest as a source of nanomaterials (i.e. nanocellulose), which combine the previously mentioned intrinsic benefits of celluloses with additional distinguishing properties of materials with dimensions in the nanoscale (e.g. high surface-to-volume ratio, high mechanical properties, etc.). However, the production of nanocelluloses from vegetal sources implies the use of harsh chemicals to dissolve the lignin-hemicellulose matrix to release cellulose fibers in the first place, as well as top-down strategies devoted to produce cellulose nanofibrils by intensive energy-demanding mechanical treatments, or cellulose nanocrystals by hydrolysis with strong acids under strictly controlled conditions of temperature, and time (Vazquez et al., 2015). On the other hand, bacterial nanocellulose (BNC) is distinguished by its high purity and by an intrinsic unique nanofibrillar structure. Besides, BNC is also recognized for a high degree of polymerization and crystallinity, different shaping possibilities, and for the high

DOI: 10.52292/j.laar.2024.2837
Received: December 6, 2022.
Accepted: April 7, 2023.
Recommended by Diego Lomonaco.

liquid loading capacity, conformability and tunable thickness and porosity of BNC pellicles (Betlej et al., 2021; Fernandez Corujo et al., 2016; Foresti et al., 2015).

The production of BNC is generally conducted using specific bacteria, typically *Komagataeibacter xylinus* (formerly *Gluconacetobacter xylinus* and *Acetobacter xylinum*), which requires axenic conditions and strict control of fermentation variables (Dima et al., 2017). However, for certain applications, bacterial nanocellulose –in the form of nanoribbons– may be obtained from the floating pellicle developed during Kombucha tea production, in much simpler processes which do not require laboratory conditions, complex growing media or sophisticated cultivation and processing equipment.

In Kombucha homebrewing it is common that the floating pellicle produced during tea fermentation is reused (as a whole or just a part of it) as inoculum in a second batch. In larger scale facilities previously fermented tea –and not pellicles– is usually used as the starter for the new batch. Given the proliferation in the last years of not only classical home-scale breweries, but also growing larger-scale Kombucha enterprises, the current contribution is focused on valorizing the cellulosic Kombucha tea by-product by isolating KBNC from the floating pellicle and using it in the production of polymeric biocomposites based on poly(lactic acid) (PLA). PLA is a currently widely used commercial thermoplastic polyester derived from biomass which can be biologically degraded under compost conditions. In recent years BNC produced by *K. xylinus* has been successfully assessed as reinforcing material of PLA (Ávila Ramírez et al., 2019, 2020; Blaker et al., 2014; Gitari et al., 2019; Luddee et al., 2014). However, the use of bacterial nanocellulose isolated from Kombucha production has been much less explored (Arteaga-Ballesteros et al., 2020). In this work, PLA nanocomposites with varying KBNC content were developed by melt compounding followed by compression molding, and they were characterized in terms of their morphology and mechanical properties.

2. Methods

2.1 Materials

Commercial black tea bags were purchased from Green Hills (Argentina). Glucose (Xantana, Argentina), potassium hydroxide (Cicarelli, Argentina) and potassium bromide (Stanton, Argentina) were all of analytical grade. The initial starter Kombucha culture was kindly provided by Aloja Fermentos (Argentina). For the development of composites, commercial PLA (Nature Works®, trade name 4043D) with a density of 1.24 g/cm^3 and a melt flow index (MFI) of 6 g/10 min (210 °C, 2.16 kg) was employed as the matrix.

2.2 Production of pellicles

Black tea infusion (10 g per liter of boiling water) was prepared and sweetened with 60 g/L of glucose. After 30 minutes tea bags were removed, and after cooling up to 25 °C, 10 % v/v of the starter culture (previously fermented Kombucha tea batch used as inoculum) was added. Containers were covered to avoid contamination but guaranteeing proper air flow, and they were kept in static conditions at 28-30 °C for 14 days. After this period the floating pellicles developed at the air-liquid interface were carefully removed and purified as detailed below.

2.3 Purification

The produced pellicles were purified using three different procedures: in treatment A) the pellicles were thoroughly washed with tap water at ambient temperature, grinded with a kitchen blender for 4 min and extensively washed with distilled water. In treatment B) after several washings with tap water pellicles were immersed in NaOH 0.5 M at 70 °C for 4 h, and then blended and washed with distilled water until neutral pH (Oliver-Ortega et al., 2021). Finally, in treatment C) thoroughly washed pellicles were blended in KOH 0.9 M for 4 min, left in alkali for 14 h at room temperature, and rinsed with distilled water until neutral pH (Ávila Ramírez et al., 2014). According to the purification procedure used, the treated pellicles were named KBNC-A, KBNC-B and KBNC-C.

2.4 Characterization of pellicles and KBNC

Environmental scanning electron microscopy (ESEM): fragments of the unpurified pellicles and drops of diluted aqueous suspensions of KBNC samples were dried (1 h, 110 °C), sputtered coated with a thin layer of gold and analyzed in a FEI Quanta 200 microscope at an accelerating voltage of 15 kV.

Transmission electron microscopy (TEM): drops of diluted aqueous suspensions of KBNC samples were negatively stained with 2 wt. % uranylacetate and observed in a TEM Philips EM 301 microscope at an accelerating voltage of 40 kV.

Fourier transform infrared spectroscopy (FTIR): milled dried samples (4 h, 110 °C) and dried KBr (overnight, 110 °C) were mixed at a 1:20 ratio, pressed into discs at 8 kg/cm^2 and dried again during 2 h at 110 °C. Samples were then placed in an Affinity-1 Shimadzu Fourier Transform Infrared Spectrophotometer and spectra were recorded in the range of 4000 and 800 cm^{-1} with a total of 32 scans at a resolution of 4 cm^{-1}. Baselines were corrected and normalized against the intensity of the absorption at 1165 cm^{-1} related to the (C–O–C) links of cellulose (Ilharco et al., 1997).

Thermogravimetric analysis (TGA): milled samples (3-5 mg) were dried for 2 h at 110 °C and analyzed in a TGA-50 Shimadzu instrument by heating from 25 °C to 800 °C at 10 °C/min under inert nitrogen atmosphere (30 mL/min). T_{onset} values were determined as the temperature of 10 % weight loss after moisture removal, and T_{max} values were obtained from the maxima of DTG curves.

X-ray diffraction analysis (XRD): X-ray diffraction patterns of milled samples were collected with a Rigaku D/Max-C Wide Angle Automated X-ray diffractometer with vertical goniometer, using Cu/Kα radiation source (0.154 nm) at 40 kV and 30 mA. The diffractograms were recorded in a 2θ interval of 10–40° at a step size of 0.02°. The crystallinity index (CrI) of KBNC samples was calculated by use of Segal's empirical equation (Eq. 1)

(Segal et al., 1959):

$$CrI(\%) = (I_{002} - I_{am})/I_{002} \times 100 \quad (1)$$

where I_{002} (maximum intensity of the 002 lattice diffraction) represents both crystalline and amorphous material, and I_{am} (intensity at 2θ = 18°) accounts for amorphous material.

2.5 Development of PLA/KBNC composites

Composites were prepared by melt mixing followed by compression molding. With this purpose, dried KBNC-C was thoroughly milled to obtain a powder (particle size distribution data are shown in Section 3.3), dried at 110 °C for 2 h and mixed with PLA pellets (previously vacuum dried at 80 °C for 4 h) using a Brabender intensive mixer operated at 170 °C and 50 rpm for 8 min. For the neat PLA sample, 50 g of pellets were melt compounded; whereas for composite samples KBNC-C powder and PLA pellets were mixed at final concentrations of KBNC-C of 1, 3, 5 and 7 wt. %. After intensive mixing, samples were vacuum dried at 80 °C for 4 h and compression molded in a hydraulic press (Carver 3853) which was kept at 170 °C with no pressure for 8 min, followed by 5 min at 2 MPa and 170 °C.

2.6 Characterization of PLA/KBNC composites

Environmental scanning electron microscopy (ESEM): Cryo-fractured surfaces of PLA and PLA/KBNC composite films were sputtered coated with a thin layer of gold and analyzed in a FEI Quanta 200 microscope at an accelerating voltage of 15 kV.

Mechanical tests: uniaxial tensile tests were performed on dumbbell samples (at least five per system) cut out from the PLA matrix and from the PLA/KBNC composites films in an INSTRON dynamometer 5985 at a crosshead speed of 5 mm/min, using a load cell of 1 kN, in accordance with the ASTM D638 standard recommendations. Average Young's modulus, tensile strength and strain at break values, as well as their deviations were determined from the obtained stress–strain curves.

3. Results

3.1 Production of pellicles

Literature review shows that Kombucha production is generally carried out using tea and sugar concentrations (%, w/v) of ≈ 0.5-1 % and 5-10 %, respectively. In reference to inoculum, both floating pellicles from a previous batch (complete or a fraction of them) and/or specified volumes (10-20 % v/v) of previously fermented tea broth can be used (da Silva Júnior et al., 2022). Regarding fermentation intervals and temperatures, most contributions refer to cultivation during 7-20 days at 18-30 °C (Coelho et al., 2020; Kim and Adhikari, 2020; Laavanya et al., 2021). Under the conditions chosen in this contribution (Section 2.2), after 14 days of fermentation pellicles with the cross-section area of the containers, thicknesses of ≈ 10 mm and ≈ 5 wt. % solid content, as the one shown in Fig. 1 were obtained. The pellicle exhibits a brownish color which has been previously attributed to the presence of melanoidins resulting from Maillard reaction between the amino groups of proteins and the carbonyl groups of reducing sugars (Dima et al., 2017; Wang et al., 2011).

Figure 1: Floating pellicle developed at the air-liquid interface during Kombucha tea production.

3.2 Characterization of pellicles and KBNC

ESEM images of the unpurified floating pellicles harvested from the tea broth surface are shown in Fig. 2 (first row). There, in accordance with previous reports (Dima et al., 2017; Ramírez Tapias et al., 2020; Sharma et al., 2019), some bacterial cells and typical micrometric-in-length and nanometric-in-width entangled bacterial cellulose ribbons embedded within a continuous matrix can be distinguished.

Purification of the harvested pellicles aimed at removing non-cellulosic residues and microorganisms was performed by three different methods, i.e. A, B and C. Due to the swelling capacity of cellulose, in all cases gel-like KBNC samples with solid contents of 1.0-1.5 wt. % were

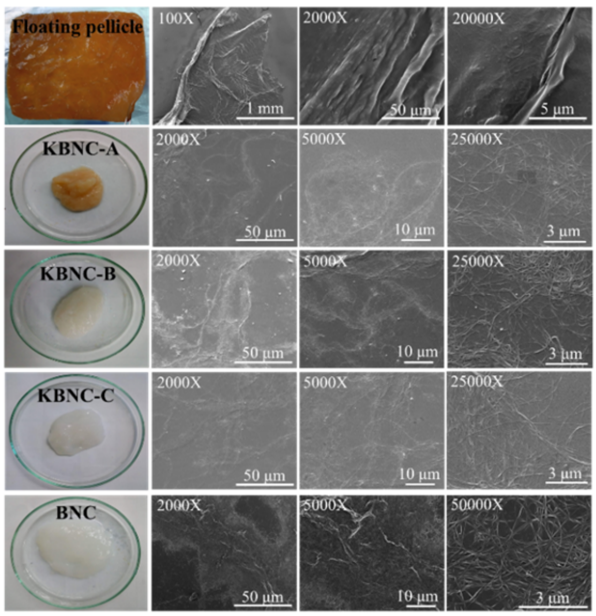

Figure 2: Photographs and ESEM micrographs of the unpurified floating pellicle developed during Kombucha production, KBNC samples recovered after purification of the pellicle with treatment A, B and C; and BNC produced by *K. xylinus*.

obtained. Figure 2 (first column) collects photographs of the different samples, evidencing significant changes in their color depending on the purification method used. The progressive reduction in the brownish color of the samples has been previously associated with the removal of melanoidins (Dima et al., 2017). ESEM micrographs of the purified samples included in the same figure show the characteristic entangled bacterial cellulose nanoribbons. Bacterial cells can still be observed especially in the KBNC sample recovered from treatment A.

The FTIR spectrum of the unpurified pellicle (Fig. 3, upper spectrum) exhibits absorbances typical of bacterial cellulose such as those found in the 3600-3000 cm^{-1} region which correspond to the stretching vibration of −OH groups present in carbohydrates; bands found in the 3000-2800 cm^{-1} interval which are attributed to the stretching of C−H linkages present in methyl and methylene groups of cellulose; and minor less defined signals within the 1450-900 cm^{-1} range associated with CH_2 symmetrical bending, cellulose C−O−C bridges, C−O stretching and other absorptions typical of β-linked glucose polymers (Ávila Ramírez et al., 2014; Cerrutti et al., 2016; Coma et al., 2019; Li et al., 2009; Peltzer et al., 2018; Song et al., 2012; Wang et al., 2013).

In addition, the floating pellicle also shows other absorption bands which are not found in BNC. For instance, those observed between 1780 and 1740 cm^{-1}, which have been previously assigned to the stretching mode of the C=O linkage of esters of compounds remaining in the samples after fermentation, such as acetates (Ramírez Tapias et al., 2020); and other bands related to the presence of proteins, nucleic acids and cell residues like the ones observed within the 1560-1510 cm^{-1} range, often ascribed to −NH groups of amide II in proteins (Dima et al., 2017; Fuller et al., 2018). Finally, the absorbance centered at 1640 cm^{-1} is associated with the bending of −OH groups in adsorbed water molecules (Cerrutti et al., 2016).

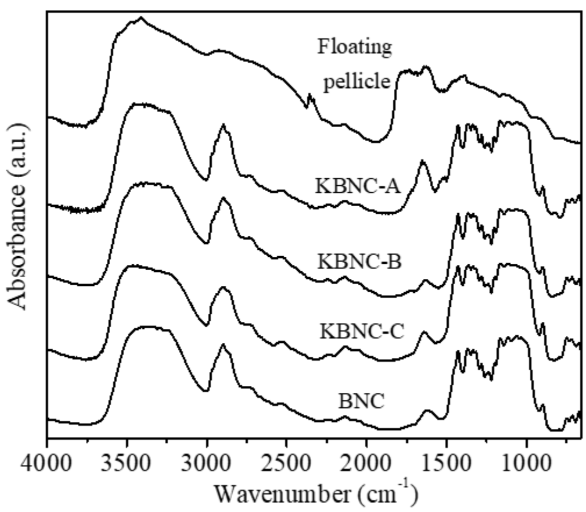

Figure 3: FTIR spectra of the unpurified floating pellicle, KBNC samples recovered from treatments A, B and C; and BNC produced by *K. xylinus*.

FTIR spectra of all KBNC samples show the aforementioned typical absorbances of bacterial cellulose. Moreover, in treatment A the absorption band associated with the stretching mode of C=O of acetate compounds (1735 cm^{-1}) (Ramírez Tapias et al., 2020), as well as the band related to −NH groups of amide II in proteins (1560-1510 cm^{-1}) described for the unpurified floating pellicle, are still visible (Dima et al., 2017), indicating that washings with water were not enough for the complete removal of fermentation residues. A very small signal centered at 1730 cm^{-1} can be identified in the spectrum of KBNC-B, which is not evident in the spectrum of KBNC-C. The implementation of the alkali treatment during/after blending the pellicles and not before blending (i.e. treatment is applied to the released micro/nanofibrils and not to the entire membrane), might have been beneficial for promoting KBNC purification in treatment C.

The thermogravimetric analysis of the unpurified pellicle is shown in Fig. 4. The corresponding weight loss curve (Fig. 4a) shows a first loss in the RT-130 °C interval which is associated with sample dehydration. The following weight loss observed in the $\approx$ 150-265 °C range has been previously ascribed to the decomposition of phenolic compounds present in the tea and remaining in the unpurified pellicle, as well as to phospholipids, proteins, nucleic acids and cellular rests derived from microorganisms (Delgado et al., 2018; Xia et al., 2015). This second weight loss accounts for 13 % of the total pellicle mass and results in a wide peak in the DTG curve with a maximum decomposition rate temperature centered at 230 °C (Fig. 4b). For the unpurified pellicle the T_{onset} value was 237 °C. A third weight loss of 52 % is observed in the $\approx$ 280-400 °C interval with a T_{max} value of 357 °C, which is associated with the main decomposition process of cellulose (Cerrutti et al., 2016; Ramírez Tapias et al., 2020).

TG and DTG data of KBNC and BNC samples are also collected in Fig. 4. From the weight loss curves (Fig. 4a), it can be observed that BNC and all treated samples present two decomposition events: a first one resulting in a weight loss of about 4 % from ambient conditions up to 130 °C associated with samples dehydration (Cerrutti et al., 2016), followed by a large weight loss which occurs mainly within the 220-400 °C range, attributed to cellulose decomposition (Ramírez Tapias et al., 2020; Vazquez et al., 2013). As expected, the percentage weight loss associated with this event is much larger for purified KBNC samples than for the original pellicle. Besides, KBNC-B and KBNC-C exhibit higher T_{onset} and T_{max} values than KBNC-A, with values typical of BNC (340 °C and 370-380 °C, respectively). Regarding temperature decomposition from 400 °C to 750 °C, residual mass values in KBNC derived from treatments B and C are similar to those collected for BNC. On the other hand, high-temperature decomposition for KBNC-A resembles that of the floating pellicle, suggesting the presence of thermally stable impurities in this sample.

Finally, Fig. 5 collects the X-ray diffractograms of all samples (unpurified pellicle, purified KBNC samples and

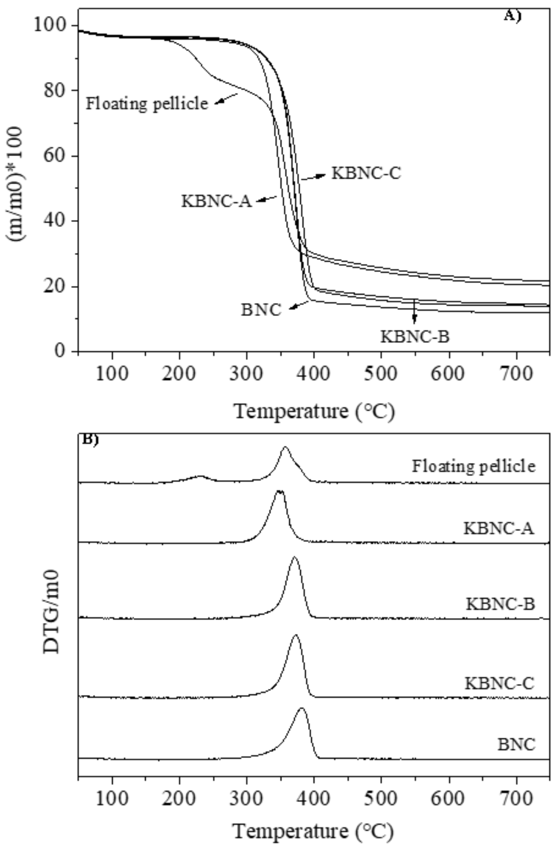

Figure 4: A) TG and B) DTG curves of the unpurified floating pellicle, KBNC samples recovered from treatments A, B and C; and BNC produced by *K. xylinus*.

BNC). In all of them three main diffraction peaks centered at 2θ = 14.4° (101), 16.7° (10-1) and 22.5° (002) can be identified. Much less intense signals at 20.1° (021) and 34.4° (040) can also be observed. These five peaks are all characteristic of cellulose I (Arteaga-Ballesteros et al., 2020; Ford et al., 2010) which is the cellulose polymorph present in BNC. Segal's empirical method for crystallinity index (CrI) calculation was applied to KBNC and BNC, resulting in all cases in high CrI values within the 84-86 % range, in accordance with previously reported values (Goh et al., 2012; Oliver-Ortega et al., 2021). These relatively high crystallinity values are characteristic of bacterial cellulose (Moon et al., 2011; Cerrutti et al., 2016) which is especially recognized among cellulose sources for its high crystallinity index. On the other hand, the diffractogram of the unpurified pellicle evidences a less crystalline pattern when compared to KBNC and BNC samples, in agreement with the presence of less crystalline impurities remaining from culture media (Dima et al., 2017; Sederavičiūtė et al., 2019).

Overall, the results from ESEM, FTIR, TGA and DRX summarized in the previous paragraphs indicate that alkali treatment of the pellicles produced as by-product of Kombucha tea fermentation allows easy isolation of bacterial cellulose nanofibrils, whose morphology, chemical structure, thermal decomposition pattern and X-ray diffractogram resemble that of the BNC obtained with the

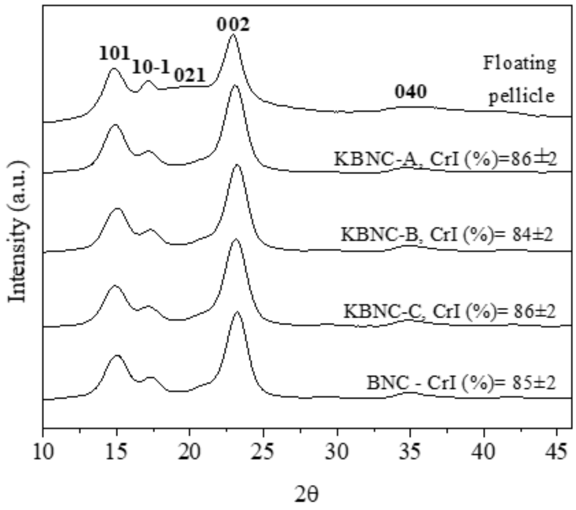

Figure 5: X-ray diffractograms of the unpurified floating pellicle, KBNC samples recovered from treatments A, B and C; and BNC produced by *K. xylinus*.

single strain of *K. xylinus* under much more demanding culture conditions. Between treatment B and C, the latter seems to be the most convenient option given not only the corresponding FTIR results, but also the fact that, –despite involving more time and alkali concentration–, no heating is needed. In view of the previous findings, KBNC-C was the one used in the production of composites with PLA. Some extra TEM images of KBNC-C nanoribbons with an average width of 77 ± 29 nm are shown in Fig. 6.

3.3 KBNC/PLA composites

The morphology of the films obtained by melt compounding of powdered dried KBNC-C (from here after simply KBNC) and PLA followed by compression molding (reinforcement content: 1, 3, 5 and 7 wt. %) are shown in Fig. 7. The particle size distribution of the powdered KBNC is also included in Fig. 7a.

Whereas PLA fracture surface presents a smooth appearance, large aggregates of dried milled KBNC can be observed in ESEM micrographs of all cryo-fractured composite samples (Fig. 7) irrespectively of the concentration of KBNC used. The aggregation of nanocelluloses upon

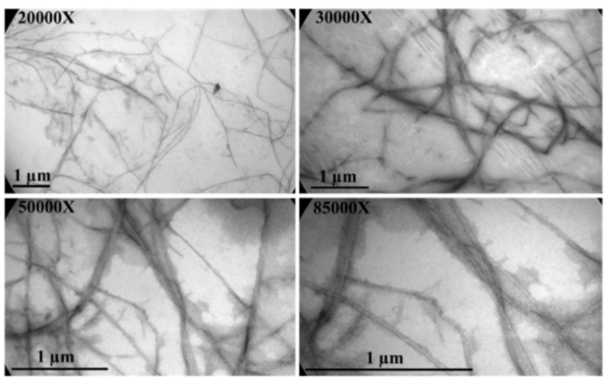

Figure 6: TEM micrographs of KBNC recovered after purification of the floating pellicle with treatment C.

drying has been previously ascribed to the high availability of -OH groups on their surface, which establish interfibrillar hydrogen bonds after the removal of water molecules. This irreversible event which is known as 'hornification' (Ding et al., 2009; Fernandes Diniz et al., 2004) compromises the nanometric scale of nano-celluloses and their derived properties. ESEM micrographs showed that the aggregation of KBNC led to a non-homogeneous distribution of the reinforcement within the PLA matrix, which resulted even more evident in composites with higher filler content which exhibited higher aggregation and rougher surfaces. Besides KBNC hornification, the limited dispersion of the reinforcement observed is also related to the relative incompatibility between PLA and KBNC due to their hydrophobic character and hydrophilic nature, respectively. The chemical incompatibility hinders filler dispersion within the matrix, and it is responsible for the poor adhesion between phases and the existence of gaps at the filler/matrix interface.

Uniaxial tensile properties of PLA and PLA/KBNC composites are shown in Fig. 8a. Results indicate that all composites exhibit Young´s modulus values higher than that of neat PLA (Fig. 8), as a result of the incorporation of a stiff filler such as nanocellulose (Panaitescu et al., 2017). Values improved for concentrations of KBNC of 1 and 3 wt. %, reaching modulus increments of 19 %, with no further significant increase at higher filler contents. This can be related to the already mentioned increase in the KBNC aggregation at higher filler loadings. On the other hand, composites tensile strength values (Fig. 8b)

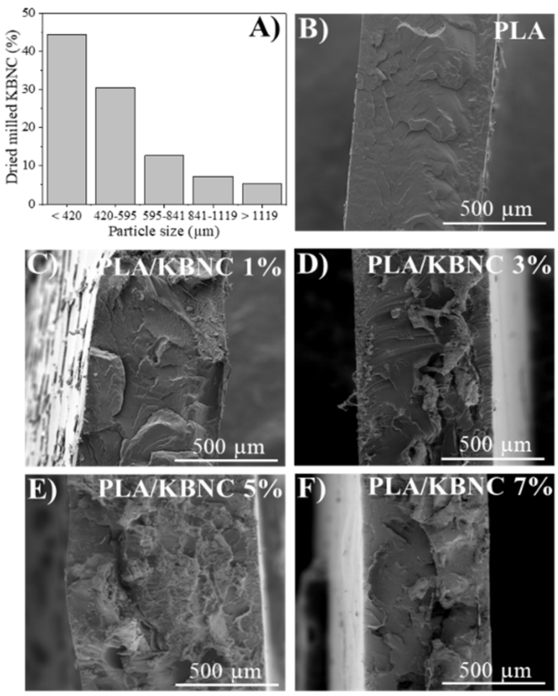

Figure 7: A) Dried milled KBNC particle size distribution and B) -F) ESEM micrographs of cryo-fractured surfaces of PLA and PLA/KBNC composite films prepared by melt compounding and compression molding (200X).

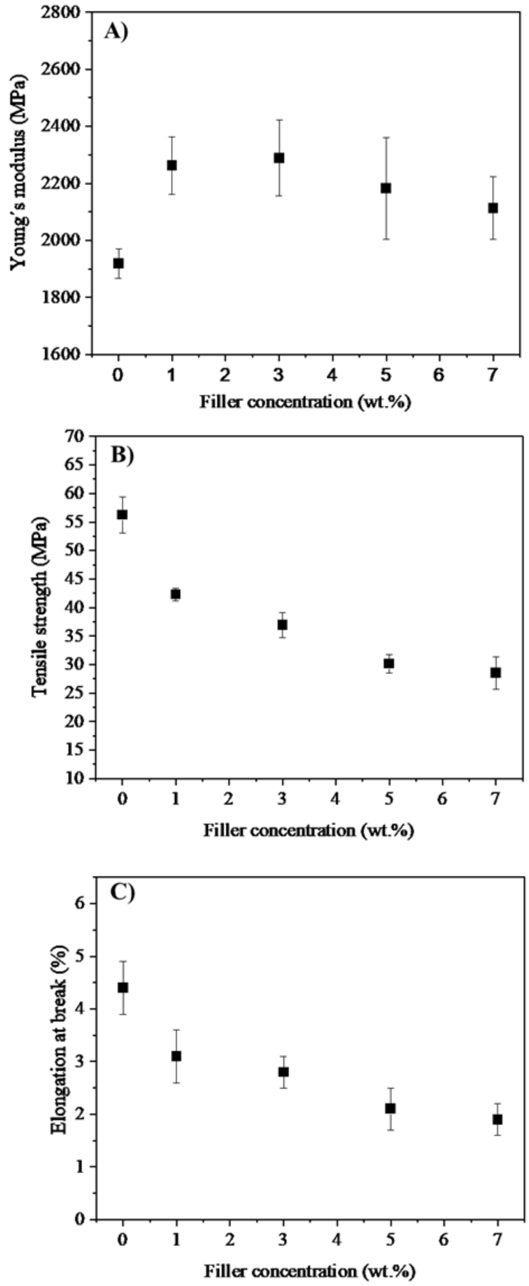

Figure 8: Tensile properties of PLA and PLA/KBNC composite films prepared by melt compounding and compression molding: A) Young´s modulus, B) Tensile strength and C) Elongation at break.

gradually decreased gradually decreased with the incorporation of KBNC. This is mainly related to a poor adhesion between the matrix and the filler (low interfacial bonding) which leads to a reduced stress transfer capacity. Also, this poor adhesion promotes the existence of voids at the fiber/matrix interface (Mathew et al., 2005).

Finally, elongation at break values are displayed in Fig. 8c. As it can be seen, these values also decreased with KBNC concentration. This is an expected trend due to the presence of nanocellulose aggregates which act as critical flows inducing premature failure (Pérez et al., 2012).

4. Conclusions

In the last years, Kombucha business has turned into one of the fastest-growing sub-segments of beverage production (especially in the United States) propelled by the growing demand for health products and natural beverage goods. Kombucha is not limited to classical home-scale breweries anymore; instead, profitable large-scale Kombucha companies have proliferated in different countries.

Given the now well-established remarkable properties of nanocelluloses and the huge variety of foreseen high-tech applications, the current contribution was focused on valorizing the cellulosic floating pellicles developed during Kombucha tea fermentation by isolation of cellulose nanofibrils. With this purpose, three different simple protocols were assayed, and purified KBNC samples were characterized in terms of morphology, chemical structure, thermal stability and crystallinity.

Overall, the results obtained showed that alkali treatments classically used for BNC (produced with the single strain of *K. xylinus*) purification were also suitable for the isolation of bacterial cellulose nanofibrils from the Kombucha by-product, whose morphology, chemical structure, thermal decomposition pattern and X-ray diffractogram resembled that of BNC obtained with *K. xylinus* under much more demanding conditions. In particular, treatment C seems the most convenient option given not only the corresponding FTIR results, but also the fact that, –despite involving more time and higher alkali concentration–, no heating was needed.

Regarding the developed PLA/KBNC composites, even if the hornification phenomenon as well as the well-known PLA-cellulose incompatibility issues severely limited the distribution and dispersion of dried KBNC-C within the PLA matrix, mechanical properties results evidenced significant increases in the stiffness of the composites for KBNC-C contents of 1 wt. % (18 %) and 3 wt. % (19 %). Considering the gradual decrease in the tensile strength values of the composites with the incorporation of KBNC, as well as reinforcement content requirements, PLA/KBNC-C composites with 1 wt. % of reinforcement seem to be the most promising candidates for further studies.

References

Andreson, M., Kazantseva, J., Kuldjärv, R., Malv, E., Vaikma, H., Kaleda, A., Kütt, M.-L., and Vilu, R. (2022). Characterisation of chemical, microbial and sensory profiles of commercial kombuchas. *Int. J. Food Microbiol.*, 373:109715.

Arteaga-Ballesteros, B. E., Guevara-Morales, A., Martín-Martínez, E. S., Figueroa-López, U., and Vieyra, H. (2020). Composite of polylactic acid and microcellulose from kombucha membranes. *e-Polymers*, 21(1):015–026.

Ávila Ramírez, J. A., Bovi, J., Bernal, C., Errea, M. I., and Foresti, M. L. (2020). Development of poly (lactic acid) nanocomposites reinforced with hydrophobized bacterial cellulose. *J. Polym. Environ.*, 28(1):61–73.

Ávila Ramírez, J. A., Cerrutti, P., Bernal, C., Errea, M. I., and Foresti, M. L. (2019). Nanocomposites based on poly (lactic acid) and bacterial cellulose acety-lated by an α-hydroxyacid catalyzed route. *J. Polym. Environ.*, 27(3):510–520.

Ávila Ramírez, J. A., Suriano, C. J., Cerrutti, P., and Foresti, M. L. (2014). Surface esterification of cellulose nanofibers by a simple organocatalytic methodology. *Carbohydr. Polym.*, 114:416–423.

Betlej, I., Zakaria, S., Krajewski, K. J., and Boruszewski, P. (2021). Bacterial cellulose–properties and its potential application. *Sains Malaysiana*, 50(2):493–505.

Blaker, J. J., Lee, K.-Y., Walters, M., Drouet, M., and Bismarck, A. (2014). Aligned unidirectional PLA/bacterial cellulose nanocomposite fibre reinforced PDLLA composites. *React. Funct. Polym.*, 85:185–192.

Cerrutti, P., Roldán, P., García, R. M., Galvagno, M. A., Vázquez, A., and Foresti, M. L. (2016). Production of bacterial nanocellulose from wine industry residues: Importance of fermentation time on pellicle characteristics. *J. Appl. Polym. Sci.*, 133(14):43109–43118.

Coelho, R. M. D., de Almeida, A. L., do Amaral, R. Q. G., da Mota, R. N., and de Sousa, P. H. M. (2020). Kombucha: Review. *Int. J. Gastron. Food Sci.*, 22:100272.

Coma, M. E., Peltzer, M. A., Delgado, J. F., and Salvay, A. G. (2019). Water kefir grains as an innovative source of materials: Study of plasticiser content on film properties. *Eur. Polym. J.*, 120:109234.

da Silva Júnior, J. C., Meireles Mafaldo, Í., de Lima Brito, I., and Tribuzy de Magalhães Cordeiro, A. M. (2022). Kombucha: Formulation, chemical composition, and therapeutic potentialities. *Curr. Res. Food Sci.*, 5:360–365.

Delgado, J. F., Peltzer, M. A., Salvay, A. G., de la Osa, O., and Wagner, J. R. (2018). Characterization of thermal, mechanical and hydration properties of novel films based on Saccharomyces cerevisiae biomass. *Innov. Food Sci. Emerg. Technol.*, 48:240–247.

Dima, S.-O., Panaitescu, D.-M., Orban, C., Ghiurea, M., Doncea, S.-M., Fierascu, R., Nistor, C., Alexandrescu, E., Nicolae, C.-A., Trică, B., Moraru, A., and Oancea, F. (2017). Bacterial nanocellulose from side-streams of Kombucha beverages production: Preparation and physical-chemical properties. *Polymers (Basel).*, 9(12):374.

Ding, J., Huang, X., Zhang, L., Zhao, N., Yang, D., and Zhang, K. (2009). Tolerance and stress response to ethanol in the yeast Saccharomyces cerevisiae. *Appl. Microbiol. Biotechnol.*, 85(2):253–263.

Dutta, H. and Paul, S. K. (2019). Kombucha drink: production, quality, and safety aspects. In Production and management of beverages. In *Prod. Manag. Beverages*, pages 259–288. Elsevier.

Fernandes Diniz, J. M. B., Gil, M. H., and Castro, J. A. A. M. (2004). Hornification. Its origin and interpretation in wood pulps. *Wood Sci. Technol.*, 37(6):489–494.

Fernandez Corujo, V., Cerrutti, P., Foresti, M., and Vázquez, A. (2016). Production of bacterial nanocellulose from non-conventional fermenta-tion media. In *Multifunct. Polym. Nanocomposites Based Cellul. Reinf.*, pages 39–59. Elsevier.

Foresti, M., Cerrutti, P., and Vazquez, A. (2015). Bacterial nanocellulose: Synthesis, properties and applications. In *Polym. Nanocomposites Based Inorg. Org. Nanomater.*, pages 39–61. John Wiley & Sons, Inc., Hoboken, NJ, USA.

Fuller, M. E., Andaya, C., and McClay, K. (2018). Evaluation of ATR-FTIR for analysis of bacterial cellulose impurities. *J. Microbiol. Methods*, 144:145–151.

Gitari, B., Chang, B. P., Misra, M., Navabi, A., and Mohanty, A. K. (2019). A comparative study on the mechanical, thermal, and water barrier properties of PLA nanocomposite films prepared with bacte-rial nanocellulose and cellulose nanofibrils. *BioResources*, 14(1):1867–1889.

Ilharco, L. M., Garcia, A. R., Lopes da Silva, J., and Vieira Ferreira, L. F. (1997). Infrared approach to the study of adsorption on cellulose: Influence of cellulose crystallinity on the adsorption of benzophenone. *Langmuir*, 13(15):4126–4132.

Jayabalan, R., Malbaša, R. V., Lončar, E. S., Vitas, J. S., and Sathishkumar, M. (2014). A review on Kombucha tea—microbiology, composition, fermentation, beneficial effects, toxicity, and tea fungus. *Compr. Rev. Food Sci. Food Saf.*, 13(4):538–550.

Kim, J. and Adhikari, K. (2020). Current trends in Kombucha: Marketing perspectives and the need for improved sensory research. *Beverages*, 6(1):15.

Laavanya, D., Shirkole, S., and Balasubramanian, P. (2021). Current challenges, applications and future perspectives of SCOBY cellulose of Kombucha fermentation. *J. Clean. Prod.*, 295:126454.

Li, J., Zhang, L.-P., Peng, F., Bian, J., Yuan, T.-Q., Xu, F., and Sun, R.-C. (2009). Microwave-assisted solvent-free acetylation of cellulose with acetic anhydride in the presence of iodine as a catalyst. *Molecules*, 14(9):3551–3566.

Luddee, M., Pivsa-Art, S., Sirisansaneeyakul, S., and Pechyen, C. (2014). Particle size of ground bacterial cellulose affecting mechanical, thermal, and moisture barrier properties of PLA/BC biocomposites. *Energy Procedia*, 56:211–218.

Mathew, A. P., Oksman, K., and Sain, M. (2005). Mechanical properties of biodegradable composites from poly lactic acid (PLA) and microcrystalline cellulose (MCC). *J. Appl. Polym. Sci.*, 97(5):2014–2025.

Oliver-Ortega, H., Geng, S., Espinach, F. X., Oksman, K., and Vilaseca, F. (2021). Bacterial cellulose network from Kombucha fermentation impregnated with emulsion-polymerized poly (methyl methacrylate) to form nanocomposite. *Polymers (Basel).*, 13(4):664.

Panaitescu, D. M., Frone, A. N., Chiulan, I., Gabor, R. A., Spataru, I. C., and Căşărică, A. (2017). Biocomposites from polylactic acid and bacterial cellulose nanofibers obtained by mechanical treatment. *BioResources*, 12(1):662–672.

Peltzer, M. A., Salvay, A. G., Delgado, J. F., de la Osa, O., and Wagner, J. R. (2018). Use of residual yeast cell wall for new biobased materials production: Effect of plasticization on film properties. *Food Bioprocess Technol.*, 11(11):1995–2007.

Pérez, E., Famá, L., Pardo, S., Abad, M., and Bernal, C. (2012). Tensile and fracture behaviour of PP/wood flour composites. *Compos. Part B Eng.*, 43(7):2795–2800.

Ramírez Tapias, Y. A., Peltzer, M. A., Delgado, J. F., and Salvay, A. G. (2020). Kombucha tea by-product as source of novel materials: Formulation and characterization of films. *Food Bioprocess Technol.*, 13(7):1166–1180.

Sederavičiūtė, F., Bekampienė, P., and Domskienė, J. (2019). Effect of pretreatment procedure on properties of Kombucha fermented bacterial cellulose membrane. *Polym. Test.*, 78:105941.

Segal, L., Creely, J., Martin, A., and Conrad, C. (1959). An empirical method for estimating the degree of crystallinity of native cellulose using the X-ray diffractometer. *Text. Res. J.*, 29(10):786–794.

Sharma, A., Thakur, M., Bhattacharya, M., Mandal, T., and Goswami, S. (2019). Commercial application of cellulose nano-composites – A review. *Biotechnol. Reports*, 21:e00316.

Song, J., Birbach, N. L., and Hinestroza, J. P. (2012). Deposition of silver nanoparticles on cellulosic fibers via stabilization of carboxymethyl groups. *Cellulose*, 19(2):411–424.

Vazquez, A., Foresti, M. L., Cerrutti, P., and Galvagno, M. (2013). Bacterial cellulose from simple and low cost production media by Gluconacetobacter xylinus. *J. Polym. Environ.*, 21(2):545–554.

Vazquez, A., Foresti, M. L., Moran, J. I., and Cyras, V. P. (2015). Extraction and production of cellulose nanofibers. In *Handb. Polym. Nanocomposites. Process. Perform. Appl.*, pages 81–118. Springer Berlin Heidelberg, Berlin, Heidelberg.

Wang, H.-Y., Qian, H., and Yao, W.-R. (2011). Melanoidins produced by the Maillard reaction: Structure and biological activity. *Food Chem.*, 128(3):573–584.

Wang, L., Dong, Y., Men, H., Tong, J., and Zhou, J. (2013). Preparation and characterization of active films based on chitosan incorporated tea polyphenols. *Food Hydrocoll.*, 32(1):35–41.

Xia, Z., Singh, A., Kiratitanavit, W., Mosurkal, R., Kumar, J., and Nagarajan, R. (2015). Unraveling the mechanism of thermal and thermo-oxidative degradation of tannic acid. *Thermochim. Acta*, 605:77–85.